TIDAL WAVES AND ONSET OF COLLECTIVITY ABOVE $N = 126$*

W. Reviol[a], D.G. Sarantites[a], X. Chen[a], M. Montero[a]
O.L. Pechenaya[b], J. Snyder[b], R.V.F. Janssens[c]
M.P. Carpenter[c], C.J. Chiara[c,d], T.L. Khoo[c], T. Lauritsen[c]
C.J. Lister[c], D. Seweryniak[c], S. Zhu[c], K. Hauschild[e]
A. Lopez-Martens[e], D.J. Hartley[f], S. Frauendorf[g]

[a]Department of Chemistry, Washington University, St. Louis, MO 63130, USA
[b]Department of Physics, Washington University, St. Louis, MO 63130, USA
[c]Physics Division, Argonne National Laboratory, Argonne, IL 60439, USA
[d]Department of Chemistry and Biochemistry, University of Maryland College Park, MD 20742, USA
[e]CSNSM, IN2P3-CNRS, F-91405 Orsay Campus, France
[f]Department of Physics, U.S. Naval Academy, Annapolis, MD 21402, USA
[g]Department of Physics, University of Notre Dame, Notre Dame, IN 46556, USA

(Received January 11, 2011)

Recent experiments in the actinide region, using Gammasphere and the evaporation residue detector HERCULES, have covered the territory between $N = 126$ and the center of static octupole deformation at $N = 134$. The ^{220}Th nucleus and the neighboring ^{218}Ra and ^{219}Th nuclei mark the emergence of quadrupole–octupole collectivity in this mass region. Their octupole bands have $B(E1)/B(E2)$ ratios which are typical for the region, but the level spacings do not concur with a rotational-like behavior. In addition, a spin-dependent staggering of the $B(E1)/B(E2)$ ratios is evident. These features can be described, based on a phonon picture, by a constant-frequency tidal-wave mode for a reflection-asymmetric nuclear surface.

DOI:10.5506/APhysPolB.42.671
PACS numbers: 27.80.+w, 27.90.+b, 23.20.Lv, 21.60.Ev

1. Introduction

Indications of the onset of octupole collectivity in the actinide region just above magic neutron number $N = 126$ can be inferred, for example, from the marked difference between the level schemes of ^{218}Th [1] and ^{220}Th [2].

* Presented at the Zakopane Conference on Nuclear Physics "Extremes of the Nuclear Landscape", August 30–September 5, 2010, Zakopane, Poland.

The $N = 128$ isotope exhibits a single $E2$ sequence with decreasing energy spacings between levels as a function of spin. This behavior is attributed to excitations associated with the $(g_{9/2})^2$ valence-neutron multiplet. In contrast, the yrast structure of the $N = 130$ isotope consists of a sequence of successive even- and odd-spin states with alternating parity, similar to those of the heavier even-mass isotopes. In the latter case, the spacing corresponding to the $E2$ transitions is approximately constant, a behavior that has been interpreted as due to a reflection-asymmetric tidal wave moving over the nuclear surface [2]. In the heavier isotopes, the spacing increases with spin, resembling rotational motion. It is carried by a combination of the collective quadrupole and octupole modes, of which $B(E1)/B(E2)$ ratios of transition probabilities of the order of 10^{-6} fm^{-2} are a benchmark.

In the odd-mass thorium isotopes, alternating-parity structures that meet the above $B(E1)/B(E2)$ benchmark are found already three mass units away from $N = 126$ *viz.* in ^{219}Th [3]. Moreover, in this nucleus parity doublets (see Sec. V.D.1 of Ref. [4]) are observed and the implications are twofold. First, the observation suggests that ^{219}Th shares more similarities with ^{223}Th than with the next heavier isotope, ^{221}Th, and an explanation has been provided based on the occupation of specific K orbitals in the neutron system [3]. Second, the isotone of ^{219}Th, ^{217}Ra [5] has only one alternating-parity structure. This difference between isotones is understood as resulting from the increase with proton number Z of the softness of the octupole mode for $Z \geq 90$ (see Fig. 7 of Ref. [4]). It also emphasizes that the Th isotopes are excellent cases for studying octupole collectivity.

Traditionally, the collective degrees of freedom have been described as static quadrupole-octupole deformation [4]. Recently, Ref. [6] argued that an interpretation in terms of the condensation of octupole phonons may be more appropriate. Additional experimental evidence for the latter has been presented in Refs. [7,8]. In this framework, the reflection-asymmetric tidal-wave and octupole-condensation pictures are manifestations of the same physics mechanism.

This paper presents results from γ-ray spectroscopic work in this mass region along with a discussion that further strengthens the above phonon picture. A study of the spin-dependent staggering of the $B(E1)/B(E2)$ ratios that has been first pointed out in the ^{220}Th case [2] is presented. New experimental information is reported for ^{221}Th and ^{218}Ra. The experiments were performed at the ATLAS accelerator at Argonne National Laboratory, with a combination of the Gammasphere [9] and HERCULES [10] detector arrays. The HERCULES array is ideal for spectroscopic work in this region, using very asymmetric heavy-ion fusion reactions [2, 11], and provides a means to separate the γ rays of the evaporation residues (ERs) from those of the dominant fission products and other sources of background.

2. Experiments and analysis

The nuclei of interest were populated via xn or αxn evaporation in the 128-MeV ^{26}Mg + ^{198}Pt $\rightarrow$ ^{224}Th* and 96-MeV ^{18}O + ^{207}Pb $\rightarrow$ ^{225}Th* reactions and the pertinent information about the experiments is summarized in Table I. When used with HERCULES, Gammasphere comprises 98 HPGe-BGO modules. It is worth mentioning that HERCULES has 64 detectors, arranged in 4 rings, and that the inner ring was partially collimated. In the ^{18}O + ^{207}Pb experiment, an improved version of HERCULES was used [12]. The main difference with respect to the ^{26}Mg + ^{198}Pt experiment was a lower ER kinetic energy and, accordingly, a rather long Time-of-Flight. Scattered beam particles traveled the flight path in $\sim$ 10 ns and beam bursts of ATLAS are nominally separated by 82.5 ns. The beam was swept in the ^{18}O + ^{207}Pb experiment to avoid having the ERs arrive at a HERCULES detector at the same time as the next beam burst. The sweeping allowed a hardware veto of scattered beam and fission events.

TABLE I

Objectives and conditions of the experiments introduced in the text.

	^{26}Mg + ^{198}Pt	^{18}O + ^{207}Pb
Nuclei of interest	^{220}Th, ^{219}Th[a]	^{221}Th, ^{218}Ra[b]
Target thickness	0.88 mg/cm^2	0.47 mg/cm^2
Beam intensity	3 pnA	6 pnA
Beam period	82.5 ns	247.5 ns[c]
HERCULES coverage[d]	$6.1^\circ \leq \theta \leq 25.5^\circ$	$6.6^\circ \leq \theta \leq 26.8^\circ$
Flight path	24.1 cm	23.2 cm
Time-of-Flight range ERs	65–90 ns[e]	91–126 ns[e]
Trigger condition	GS[f] only	GS[f], HERCULES

[a]The ER channels are $4n$ and $5n$, respectively.
[b]The ER channels are $4n$ and $\alpha 3n$, respectively.
[c]One out of three ATLAS periods (beam sweeping).
[d]Polar angles with respect to the beam axis.
[e]Determined by the ER production at the beginning or end of the target.
[f]Abbreviation for Gammasphere.

The γ rays from ER nuclei were selected by two-dimensional gating on the HERCULES parameters time-of-flight and pulse height. The energies of these γ rays were corrected for Doppler shift by using the observed ER direction. Finally the γ-ray coincidences and angular distributions were analyzed. Examples of ER-gated γ-ray coincidence spectra from the ^{18}O + ^{207}Pb experiment are shown in Fig. 1.

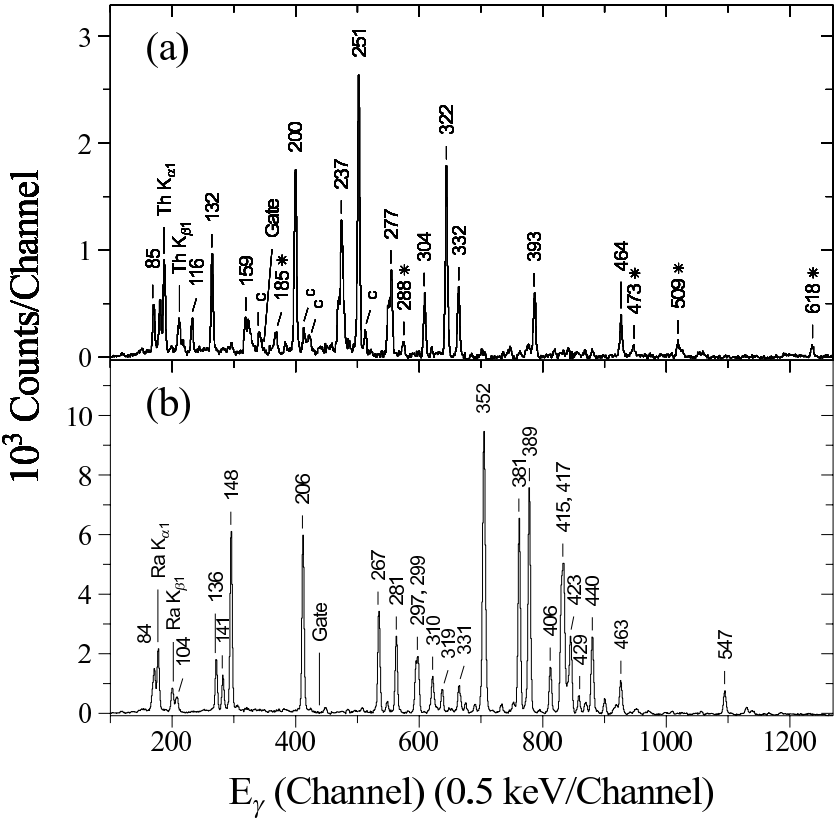

Fig. 1. Sample ER-gated γ-ray coincidence spectra for (a) ^{221}Th and (b) ^{218}Ra from the ^{18}O + ^{207}Pb experiment. The gating transitions have energies of 174 keV (^{221}Th [13]) and 219 keV (^{218}Ra [14]). The ^{221}Th transitions in spectrum (a) marked with an asterisk are newly observed. Contaminant peaks in spectrum (a), labeled "c", are from ^{222}Th and are attributed to ^{208}Pb target impurities.

The goal of this experiment was a study of ^{221}Th. Dahlinger *et al.* [13] demonstrated that ^{221}Th has not the parity-doublet behavior of ^{223}Th. Hence, it remains important to delineate the non-yrast structure of ^{221}Th. The spectrum gated by the low-lying 174-keV $(I_0 + 5^-) \rightarrow (I_0 + 4^+)$ transition, where I_0 is the ground-state spin [13], is representative for the yrast octupole band, which has been extended [15]. Among the newly observed γ rays shown in this spectrum, the 185- and 618-keV lines are transitions from non-yrast states, the latter transition being a direct link to the yrast band. The study of ^{218}Ra provides new information on $B(E1)/B(E2)$ ratios in this $N = 130$ nucleus and Fig. 1 (b) shows the quality of the data.

3. Results

3.1. N = 130 isotones

The ^{220}Th level scheme, established in the ^{26}Mg + ^{198}Pt experiment, has the following features: First, alternating-parity structures persist up to the highest spins observed, but the nucleus exhibits a vibrational-like behavior. Second, two odd-spin, negative-parity $E2$ sequences, labeled "a" and "b" in Fig. 4 of Ref. [2], are present (and a non-yrast even-spin, negative-parity sequence). Third, the $B(E1)/B(E2)$ ratios stagger as a function spin. The first and second feature is shown in Fig. 2. The yrast states of ^{220}Th have an approximately constant rotational energy $\hbar\omega \simeq \mathrm{E}_\gamma/2$. The isotone ^{218}Ra [14] shows a very similar behavior, which is in contrast to the $N \geq 132$ isotones and which indicates that these $N = 130$ nuclei do not rotate faster to acquire angular momentum. The third feature is shown in the top-left panel of Fig. 3. For $I < 14$, the $B(E1)/B(E2)$ ratios for the odd-spin states (negative parity) lie systematically lower than the ratios for the even-spin states (positive parity). In Ref. [2], the deviating data point for the 13^-_1 state was attributed to a loss of $E2$ strength at the backbending of the sequence (*cf.* Fig. 2). The $B(E1)/B(E2)$ ratio for the 13^-_2 state is smaller, but in line with the staggering effect. For $I \geq 14$, no staggering effect is recognized. This may be attributed to the spread of $E1$ strength due to the presence of two 13^- and 15^- final states.

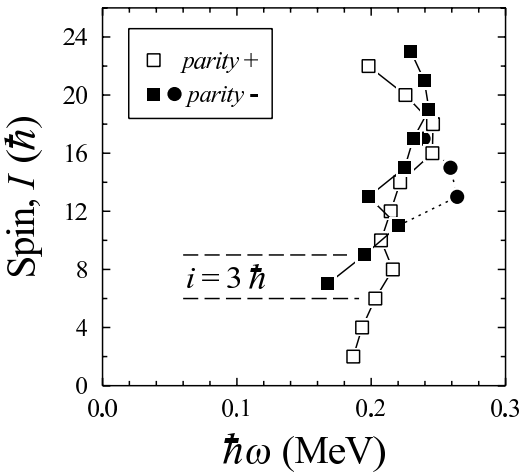

Fig. 2. Initial spin I *vs.* rotational energy $\hbar\omega$ for the near-yrast $E2$ sequences in ^{220}Th [2]. A distinction between positive- and negative-parity sequences is made using open and full symbols, respectively. The dashed horizontal lines indicate an initial alignment i close to $3\hbar$ of the yrast negative-parity sequence (see Sec. 4.1).

The $B(E1)/B(E2)$ ratios for ^{218}Ra, obtained from the ^{18}O + ^{207}Pb data, are shown in the top-right panel of Fig. 3. The ratios stagger with the same phase as in the ^{220}Th case and the effect occurs for $9 \leq I \leq 14$. The plot of $B(E1)/B(E2)$ ratios for ^{218}Ra appears to be smoother than the corresponding ^{220}Th data. This seems to be expected, since a backbending and a second odd-spin, negative-parity sequence are unique for ^{220}Th [2]. Another observation is that the staggering effect in ^{218}Ra starts two units higher in spin than in the ^{220}Th case.

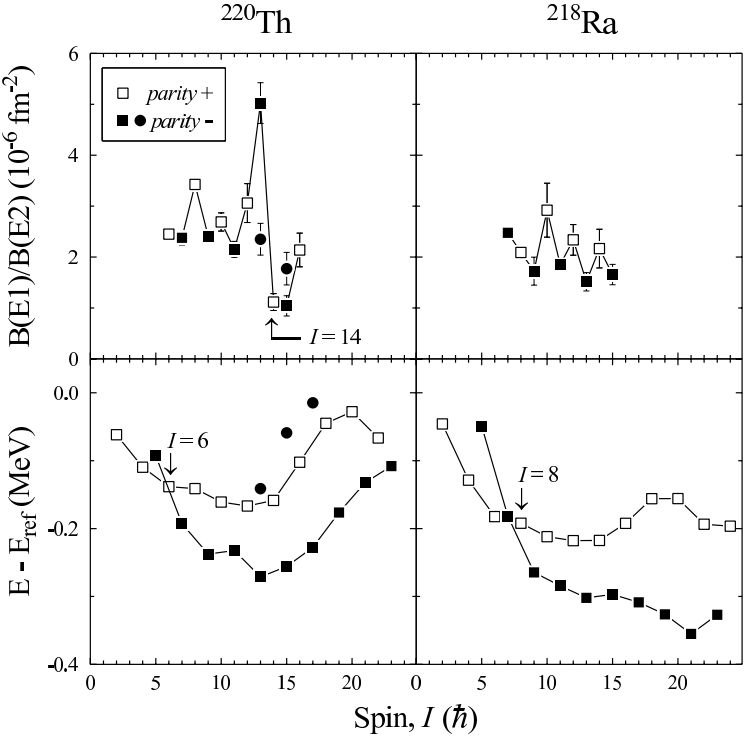

Fig. 3. $B(E1)/B(E2)$ ratios (top) and energies E–$E_{\rm ref}$ (bottom), as a function of spin I, for occtupole-type structures in ^{220}Th and ^{218}Ra. The values for the sets of yrast states with opposite parity are connected, those for the yrare states are not. The reference energy used in the bottom plots is defined as $\mathrm{E_{ref}} = 5/23$ MeV I (see Sec. 4.1). The E–$E_{\rm ref}$ *vs.* I plot for ^{218}Ra has been truncated at $I = 24$.

3.2. Odd-mass thorium isotopes

The ^{219}Th level scheme, established in the ^{26}Mg + ^{198}Pt experiment, has as key feature two parallel structures of alternating-parity levels assigned to $s = \pm i$ [16]. The level scheme is important for both the emergence

of quadrupole-octupole collectivity in this region and the trend for parity-doublet bands. The "simplex bands" in ^{219}Th have $B(E1)/B(E2)$ ratios of the same order of magnitude as those in the heavier thorium isotopes. For the $s = -i$ and $+i$ structures, the average value of these ratios is $1.2(2)\times10^{-6}$ fm^{-2} and $2.4(9) \times 10^{-6}$ fm^{-2}, respectively. The decay sequences are rather short and, thus, do not add to the systematic study of reduced transition probabilities as a function of spin. Nevertheless, since their level-energy spacings are not rotational-like they are in line with the features of ^{220}Th.

The parity-doublet aspect implies that the pairs of states with the same spin, but opposite parity, are nearly degenerate in energy. In ^{219}Th, the lowest four pairs differ in energy between −125 keV and +61 keV, *i.e.*, the energy differences fluctuate around 0 and none of the $s = \pm i$ structures is energetically favored over the other. For comparison, in the ^{223}Th case the energy differences vary between −61 keV and +31 keV. In this regard, the two nuclei are similar indeed.

The yrast octupole band in ^{221}Th is fed by rather high-energy transitions such as the 618-keV line reported in Sec. 2. An excited octupole band in ^{221}Th has been identified which is elevated by about 400 keV relative to the yrast band [15]. At this point, the ^{221}Th case serves as a contrast to the parity doubling seen in ^{219}Th and ^{223}Th.

4. Discussion

4.1. Tidal-wave interpretation

In Ref. [2], it was pointed out that the ^{220}Th and ^{218}Ra features do not fit in a traditional nuclear-rotation framework, nor can they reflect the presence of spherical vibrational phonons. Instead an approach was proposed which considers collectivity arising from reflection-asymmetric nuclear tidal waves, hereby retaining the structure of an octupole band. The nuclear shape in the rotating frame of reference is a combination of quadrupole and octupole deformations which both increase with spin. The concept of tidal waves accounts for the features described in Sec. 3.1 as follows.

Vibrational-like behavior of I vs. $\hbar\omega$. Figure 3 (bottom) shows that the yrast energies deviate by less than 300 keV from the linear function $E_{\rm ref}(I) = 5/23$ MeV I. Notably, this near-linear spin dependence concurs with the near-vertical function $I(\omega)$ shown in Fig. 2. The tidal wave travels with a constant angular velocity ω. The angular momentum increases because the wave amplitude in the quadrupole-octupole degrees of freedom increases along the yrast line. Following Ref. [6], the increase of the amplitude is accomplished by stacking aligned quadrupole and octupole phonons carrying $2\hbar$ and $3\hbar$ of angular momentum, respectively. The parity of the state is determined by the the number n of octupole phonons. Only states with

even n or odd n mix. The positive-parity $E2$ sequence starts with the $n = 0$ state, and the negative-parity sequence with $n = 1$ and, as indicated in Fig. 2, with an initial alignment $i \approx 3\hbar$. Both sequences are built up, in steps of $2\hbar$, by stacking quadrupole phonons. However, the quadrupole phonons are in ^{220}Th and ^{218}Ra less collective than in the respective heavier isotopes, as suggested by the deformation trend with N. This allows for the fact that the stacking of octupole phonons becomes competitive with the quadrupole mode as spin increases. The combined stacking of quadrupole and octupole phonons results in the near-linear spin dependence of the excitation energy noted above. In addition, a reduced quadrupole collectivity allows for the alignment of individual nucleon spins that may have caused the backbending seen in ^{220}Th. Such an irregularity is also found in the quadrupolar tidal-wave sequences of some cadmium nuclei around mass 110 [17]. Classically, the combined-phonon stacks correspond to a heart shaped wave running over the nuclear surface [6].

Spin-dependent staggering of B(E1)/B(E2) ratios. The $B(E1)/B(E2)$ ratios can be used as a probe of the competition between quadrupole- and octupole-phonon excitations. In the absence of absolute $B(E1)$ and $B(E2)$ values for ^{220}Th, we assume that the staggering effect is due to a variation of the $B(E1)$ value with spin. Using the fact that the total angular momentum is the sum of the angular momentum S of the octupole phonons and R of the quadruple phonons, a rule for the $E1$ transitions has been put forward: the transition $n \to n - 1$, where S and R change by -3 and 2, respectively, is favoured over the transition $n \to n + 1$, where S and R change by 3 and -4, respectively, because of the larger change of R [6]. The staggering of the $B(E1)/B(E2)$ ratios can then be related to a change in the phonon configuration of the positive-parity $E2$ sequence from $n = 0$ to $n = 2$ around $I = 6$. The corresponding change in ^{218}Ra occurs around $I = 8$. Here, a change in the staggering phase is seen which can be interpreted as an admixture of the $n = 0$ and 2 configurations. In the ^{220}Th case, the negative-parity sequence preserves its $n = 1$ character at least up to $I = 13$. However, the 13^-_2 state represents the continuation of the $n = 1$ configuration in the region of the backbending. The 13^-_1 state is associated with a rearrangement of individual nucleon spins, like in the mass 110 cases.

A comment about the initial alignment is in order. A value close to the limit of $3\hbar$ is only observed at $N = 130$. For higher N, $i \lesssim 2\hbar$ is typical (see Fig. 5 of Ref. [6]). In the heavier isotopes, the positive-parity sequence seems to start with a substantial $n = 0$, $n = 2$ mixing, which reduces the angular-momentum difference with the negative-parity sequence. The $n = 0$ to $n = 2$ configuration change, on the other hand, is viewed as a response of the $N = 130$ nucleus to an increasing angular momentum.

4.2. Properties of the odd neutron

The common characteristic of the odd- and even-mass nuclei in the light-actinide region is the appearance of low-lying positive- and negative-parity states forming octupole-type band structures. Recall that the $B(E1)/B(E2)$ ratios of the structures in ^{219}Th and ^{220}Th are similar ($\geq 10^{-6}$ fm^{-2}) and concur with those measured in the heavier isotopes. However, the recently studied odd-mass thorium isotopes differ from each other in a specific way. Whereas ^{219}Th shows parity doublets, ^{221}Th is without this feature. A related feature of ^{219}Th is the presence of low-lying $M1$ transitions connecting parts of the $s = -i$ structure with the $s = +i$ one [3].

To interpret the ^{219}Th level scheme, we refer to a neutron single-particle diagram such as in Fig. 33 of Ref. [4], where the level energies are given as a function of the quadrupole and octupole deformations. In the absence of static octupole deformation ($\beta_3 = 0$), the lowest-lying configurations at $N = 129$ are $(g_{9/2})^3$ and $i_{11/2}(g_{9/2})^2$. These give rise to the positive-parity members of the $s = +i$ and $s = -i$ bands, respectively. The coupling of these two configurations with the octupole phonon explains the corresponding negative-parity states. In addition, the $M1$ transitions indicate that the angular momentum must have a component within the symmetry plane. This tilt of the rotational axis generates the parity doublets by breaking the simplex symmetry (see Sec.VI.B of Ref. [18]).

The tilt can be associated with the occupation of a $K = 3/2$ orbital, using the single-particle diagram for a small deformation $\beta_2 < 0.1$. This should be contrasted by the case of ^{221}Th ($N = 131$). For a moderate deformation $\beta_2 \sim 0.1$, the odd neutron occupies a $K = 1/2$ orbital, consistent with an $i_{11/2}(g_{9/2})^4$ ground-state configuration of ^{221}Th [13]. For $K = 1/2$, no tilt is expected and parity doublets are absent. Hence, ^{221}Th resembles the even-mass neighbors with their $K = 0$ bands.

5. Conclusions

Octupole correlations provide a good example about how the symmetries of the rotating mean field dictate the spin-parity sequence of the level structure. The ^{218}Ra, ^{219}Th, and ^{220}Th nuclei mark the onset of quadrupole-octupole collectivity just 3–4 mass units above $N = 126$. In these nuclei, the pattern of $E1$ and cross-over $E2$ transitions is fully developed like in the heavier-mass octupole-type rotors, but the details of the level structures do not concur with that excitation mode. The $I(\omega)$ function behaves in a vibrational-like manner and $B(E1)/B(E2)$ *vs.* I staggers. These features are described in a consistent way by the tidal-wave concept.

A sub-aspect of ^{219}Th is the parity doubling found in this nucleus which leads to the following conclusion. Parity doublets occur in odd-mass and odd-Z, odd-N octupole nuclei, because there is an angular momentum component within one of the reflection planes. The exceptions are $K = 1/2$ bands (and $K = 0$ bands in even-mass nuclei) where such a component is absent, and a single alternating-parity sequence appears.

Tidal waves seem to be a rather common phenomenon in transitional regions. The present cases represent a change from non-collective behavior, associated with a spherical nuclear shape, to collective behavior, with stable quadrupole and octupole deformations. Analog cases in the regime of reflection-symmetric shapes are the "tidal" bands in the mass 110 region [17].

The authors thank J. Elson (WU) and J. Rohrer (ANL) for technical help and J.P. Greene (ANL) for making the targets. This work was supported by the U.S. Department of Energy, Office of Nuclear Physics, grant Nos. DE-FG02-88ER-40406, DE-AC02-06CH11357, and DE-FG02-95ER40934, and the National Science Foundation, grant No. PHY-0854815.

REFERENCES

[1] W. Bonin *et al.*, *Z. Phys.* **A322**, 59 (1985).
[2] W. Reviol *et al.*, *Phys. Rev.* **C74**, 044305 (2006).
[3] W. Reviol *et al.*, *Phys. Rev.* **C80**, 011304(R) (2009).
[4] P.A. Butler, W. Nazarewicz, *Rev. Mod. Phys.* **68**, 349 (1996).
[5] N. Roy *et al.*, *Nucl. Phys.* **A426**, 379 (1984).
[6] S. Frauendorf, *Phys. Rev.* **C77**, 021304(R) (2008).
[7] X. Wang *et al.*, *Phys. Rev. Lett.* **102**, 122501 (2009).
[8] S. Zhu *et al.*, *Phys. Rev.* **C81**, 041306(R) (2010).
[9] I.Y. Lee, *Nucl. Phys.* **A520**, 641c (1990).
[10] W. Reviol *et al.*, *Nucl. Instrum Methods* **A541**, 478 (2005).
[11] W. Reviol *et al.*, *Acta Phys. Pol. B* **38**, 1547 (2007).
[12] The photomultiplier readout is in air and the target-to-detector distance has been somewhat shortened reducing the flight path (*cf.* Table I).
[13] M. Dahlinger *et al.*, *Nucl. Phys.* **A484**, 337 (1988).
[14] N. Schulz *et al.*, *Phys. Rev. Lett.* **63**, 2645 (1989).
[15] W. Reviol *et al.*, to be published.
[16] For half-integer spin, the simplex s is defined as $s = p \cdot \exp(i\pi I)$, where p and I represent parity and spin, respectively.
[17] S. Frauendorf, Y. Gu, J. Sun, *Int. J. Mod. Phys.* **E**, in print.
[18] S.G. Frauendorf, *Rev. Mod. Phys.* **73**, 463 (2001).